

<sup>1</sup>E. P. Wigner, Proc. Natl. Acad. Sci. USA **22**, 662 (1936); E. Feenberg, Phys. Rev. **42**, 667 (1937); N. Kemmer, Nature **140**, 192 (1937); G. Breit and E. P. Wigner, Phys. Rev. **53**, 998 (1938); G. M. Volkoff, *ibid.* **62**, 126, 134 (1942); E. Feenberg and H. Primakoff, *ibid.* **70**, 980 (1946). For a summary, see, for instance, J. M. Blatt and V. F. Weisskopf, *Theoretical Nuclear Physics* (Wiley, New York, 1952), Chap. III [for the rectification of a detail in this review, dealing however with sufficient, rather than necessary, conditions for saturation, see F. Calogero, Yu. A. Simonov, and E. L. Surkov, Phys. Rev. C **5**, 1493 (1972)].

<sup>2</sup>(a) F. Calogero and Yu. A. Simonov, Nuovo Cimento **64B**, 337 (1969); (b) F. Calogero and Yu. A. Simonov, Lettere Nuovo Cimento **4**, 219 (1970); (c) F. Calogero, in *Problems of Modern Nuclear Physics, Proceedings of the Second Problem Symposium on Nuclear Physics, Novosibirsk, June 1970* (Nauka, Moscow, 1971), pp. 102–128; (d) F. Calogero and Yu. A. Simonov, Phys. Rev. Letters **25**, 881 (1970); (e) F. Calogero and Yu. A. Simonov, in *The Nuclear Many-Body Problem, Proceedings of the Symposium on Present Status and Novel Developments in the Nuclear Many-Body Problem, Rome, September 1972*, edited by F. Calogero and C. Ciofi degli Atti (to be published).

<sup>3</sup>See the discussion following the paper by J. W. Negele, in *Problems of Modern Nuclear Physics, Proceedings of Second Problem Symposium on Nuclear Physics, Novosibirsk, June 1970* (see Ref. 2), p. 218. See also the

papers by H. A. Bethe, Ann. Rev. Nucl. Sci. **21**, 93 (1971); V. F. Demin, Zh. Eksperim. i Teor. Fiz.–Pis'ma Redakt. **14**, 602 (1971) [transl.: JETP Letters **14**, 419 (1971)]; and Ref. 2(e) above.

<sup>4</sup>See Refs. 2(b) and 2(e) and the remark by Yu. A. Simonov after the paper of Ref. 2(c) above.

<sup>5</sup>In the course of that work advantage was also taken of a mathematical trick due to the other author of this paper (FP). Three additional researchers in Rome (E. Olivieri, O. Ragnisco, and M. Scialia) were also involved in this collaboration, although their contribution to this particular problem was quite marginal.

<sup>6</sup>These results were also presented by one of us (FC) to the Symposium on Present Status and Novel Developments in the Nuclear Many-Body Problem, Rome, September 1972 (to be published).

<sup>7</sup>A. R. Bodmer, Phys. Rev. D **4**, 1601 (1971); in *The Nuclear Many-Body Problem, Proceedings of the Symposium on Present Status and Novel Developments in the Nuclear Many-Body Problem, Rome, September 1972* (see Ref. 2).

<sup>8</sup>K. Eikemeier and H. H. Hackenbroich, Nucl. Phys. **A169**, 407 (1971).

<sup>9</sup>T. Ueda and A. E. S. Green, Phys. Rev. **17**, B1304 (1968); Nucl. Phys. **B10**, 289 (1969), hereafter referred to as UG1 and UG2. See also F. Calogero and D. Levi, Phys. Rev. (to be published).

<sup>10</sup>F. Calogero and Yu. A. Simonov, Phys. Rev. Letters **25**, 881 (1970).

## Electroexcitation of ${}^9\text{Be}$ Levels in the 14–18-MeV Region\*

J. C. Bergstrom, I. P. Auer, M. Ahmad, F. J. Kline, J. H. Hough,† H. S. Caplan, and J. L. Groh  
Saskatchewan Accelerator Laboratory, University of Saskatchewan, Saskatoon, Canada S7N 0W0

(Received 14 August 1972; revised manuscript received 5 February 1973)

The form factors for electroexcitation of the lowest  $T = \frac{3}{2}$  levels in  ${}^9\text{Be}$  (14.39 MeV,  $\frac{3}{2}^-$ ; 16.97 MeV,  $\frac{1}{2}^-$ ) have been measured for momentum transfers between 0.5 and 1.1  $\text{fm}^{-1}$ . Results are also presented for levels of unknown  $TJ^\pi$  at 16.63 and 17.48 MeV excitation. Radiative widths have been extracted. The form factor of the 16.63-MeV state is compared with simple-spherical and deformed shell-model form factors. The ground-state rms radius and quadrupole moment have been deduced from the elastic scattering data.

### I. INTRODUCTION

An interesting feature of  ${}^9\text{Be}$  and a few other light nuclei is the existence of several narrow states ( $\Gamma \lesssim 100$  keV) near 16 MeV excitation. For example, in  ${}^9\text{Be}$  there are  $T = \frac{3}{2}$  states at 14.39 ( $\frac{3}{2}^-$ ) and 16.97 MeV ( $\frac{1}{2}^-$ ), and states of unknown  $TJ^\pi$  at 16.67, 17.28, and 17.48 MeV. These levels lie well within the neutron continuum, but are either bound or slightly unbound to proton emission. The  $T = \frac{3}{2}$  levels have very narrow widths, less than 1 keV, which one expects since the isospin-conserving particle-decay channels are energetically un-

favored. The spins, isospins, and parities of the other three levels are not known, so it is not clear what mechanism is suppressing the neutron partial widths for decay to the ground and excited states of  ${}^9\text{Be}$ .

Few calculations have been made on the high-energy states of  ${}^9\text{Be}$ . The most extensive work of which we are aware is the intermediate-coupling calculation of Barker<sup>1</sup> for the states based on the  $1s^4 1p^5$  configuration. The interaction parameters were chosen to fit the excitation energies of a number of levels in  ${}^9\text{Be}$ , including the  $TJ^\pi = \frac{1}{2} \frac{5}{2}^-$  (2.43-MeV),  $\frac{1}{2} \frac{7}{2}^-$  (6.66-MeV),  $\frac{3}{2} \frac{3}{2}^-$  (14.39-MeV),

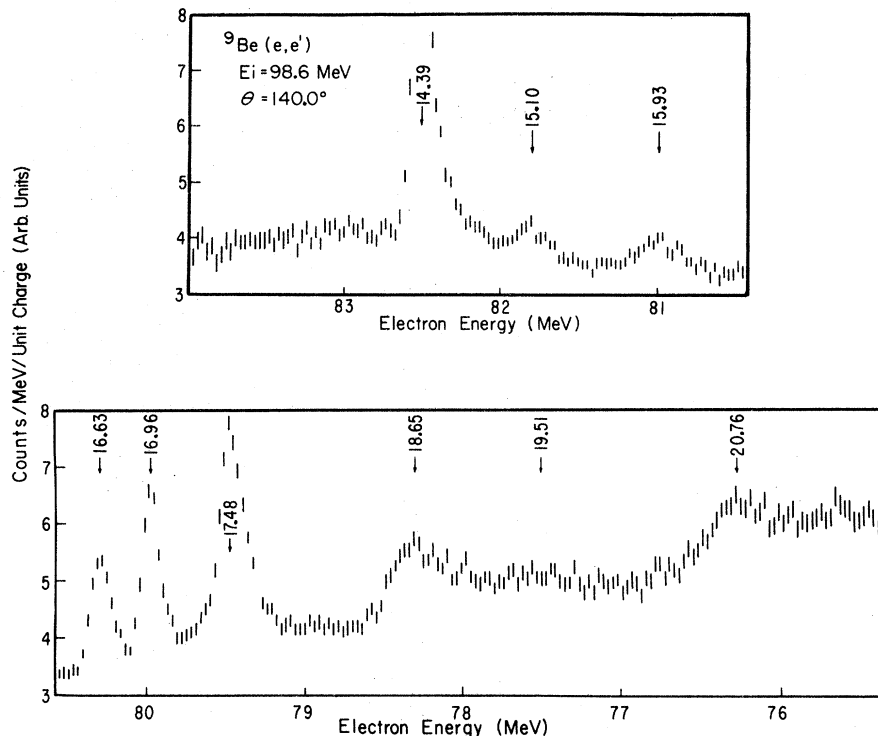


FIG. 1. Spectra of electrons inelastically scattered from  ${}^9\text{Be}$  in the 14–22-MeV excitation region. The data points are separated by 30 keV.

and  $\frac{3}{2}\frac{1}{2}^-$  (16.97-MeV) states. Four  $T = \frac{3}{2}$  levels and six  $T = \frac{1}{2}$  levels were calculated to lie between 14 and 19 MeV excitation. Five of these states have predicted ground-state radiative widths greater than 1 eV, and therefore should be readily populated by electroexcitation at favorable momentum transfers.

We have examined the 14–22-MeV region of  ${}^9\text{Be}$  using inelastic electron scattering with incident-beam energies up to 122 MeV. The strongest inelastic peaks were observed corresponding to levels at  $(14.388 \pm 0.015)$ ,  $(16.631 \pm 0.015)$ ,  $(16.961 \pm 0.015)$ , and  $(17.480 \pm 0.020)$  MeV excitation. Weaker levels were found at 13.84, 15.10, 15.93, 18.02, 18.62, 19.51, and 20.76 MeV excitation (all  $\pm 0.050$  MeV). Most of these levels have been seen in other electron-scattering work.<sup>2</sup> Figure 1 illustrates a spectra obtained in this experiment in the 14–22-MeV excitation region, while Fig. 2 shows three spectra in the 17-MeV region. Note that the 16.63-MeV peak has nearly vanished in the 122.3-MeV spectrum, implying the diffraction minimum of the form factor has been approached. The 14.388- and 16.961-MeV excitations are the lowest known  $T = \frac{3}{2}$  levels in  ${}^9\text{Be}$ , previously reported<sup>3</sup> at 14.392 and 16.973 MeV. The 16.63-MeV peak is

possibly the state reported at 16.67 MeV by Cocks<sup>4</sup> from the  ${}^7\text{Li}({}^3\text{He}, p){}^9\text{Be}$  reaction and at 16.65 MeV in the Darmstadt electron-scattering work.<sup>5</sup>

The purpose of this paper is to report measurements of the form factors for the electroexcitation of the 14.39- ( $\frac{3}{2}^-$ ), 16.63-, 16.96- ( $\frac{1}{2}^-$ ), and 17.48-MeV levels of  ${}^9\text{Be}$  at momentum transfers between 0.52 and 1.10  $\text{fm}^{-1}$ . Radiative widths have been extracted and compared with the theoretical predictions of Barker. The inelastic scattering cross sections were measured relative to the elastic cross section. The elastic form factor in turn was evaluated not by an absolute measurement, but rather by an internal-consistency method, described below.

## II. EXPERIMENTAL APPARATUS

This experiment was carried out at the electron-scattering facility at the University of Saskatchewan. The target was a wafer of metallic beryllium approximately 70  $\text{mg}/\text{cm}^2$  thick. Spectra were measured at scattering angles of 145.0, 145.9, and 153.4° and the incident-beam energy was varied between 62 and 122 MeV. The beam charge was measured by a nonintercepting resonant-toroid monitor.

Scattered electrons were detected by a recently installed 45-channel array constructed from 24 overlapping plastic scintillators arranged along the focal plane of a 20-in. radius-of-curvature  $127^\circ$  double-focussing spectrometer. A channel is defined by a multiple-coincidence requirement between adjacent detectors. The detectors are 0.35 in. wide in the dispersive plane. Each detector contributes to five channels, so the channel width is about 0.07 in., which corresponds to a momentum acceptance of about 0.08%. Details of the detector system will be published elsewhere.<sup>6</sup>

### III. ANALYSIS OF DATA

#### Elastic Scattering

Normally, absolute cross-section measurements depend on an accurate knowledge of the acceptance solid angle of the spectrometer, the target thickness, and the calibration of the charge monitor. For the present experiment, the product of these three variables was not sufficiently well determined to permit an accurate absolute measurement. Instead, the product was treated as an unknown parameter which was deduced from the data, along with the nuclear charge-distribution parameters, by a least-squares fitting procedure. This approach does not lead to precise determination of those parameters, but it does provide a consistency check with the results of previous elastic scattering experiments.

The procedure for obtaining the elastic form factor was as follows. The areas of the elastic scattering peaks were computed by integrating the spectra from the high-electron-energy side down to a point about three peak widths below the maxima. The usual virtual and soft photon (Schwinger correction), thick target bremsstrahlung, and ionization-loss correction factors were applied.<sup>7</sup> Angle- and energy-dependent kinematic factors, characteristic of the Mott cross section, were removed, leaving modified elastic peak areas which are directly proportional to the elastic scattering form factor. (Actually, the usual form-factor description is only valid in the Born approximation; for the present discussion we will define the form factor as the ratio of an experimental cross section  $d\sigma/d\Omega$  to the Mott cross section  $\sigma_M$ .)

One cannot directly compare elastic scattering cross sections with calculations based on the Born approximation, since the electron wave is distorted by the Coulomb interaction. Therefore, the data were reduced to "Born-approximation data" by multiplying the areas by distortion factors equal to the ratio of  $E0$  cross sections evaluated in the Born approximation to those computed by the phase-shift program YALERF. The shell-model charge

distribution used in evaluating the ratios had an rms radius of 2.45 fm. The  $^9\text{Be}$  elastic scattering cross section contains  $E0$  and  $E2$  terms, and we assumed the Coulomb distortion factor is the same for both.

The  $M1$  and  $M3$  contributions are  $\leq 1\%$  under the conditions of this experiment, and therefore were neglected.

Finally, the modified peak areas, corrected for Coulomb distortion, were least-squares fitted to the  $p$ -shell phenomenological function

$$A_{\text{el}} = NF^2(q),$$

$$F^2(q) = [(1 - \alpha q^2)^2 + (Q/6Z)^2 q^4] e^{-b^2 q^2/2} \quad (1)$$

to give  $N$ ,  $\alpha$ , and  $b$  for various values of  $Q$ . The

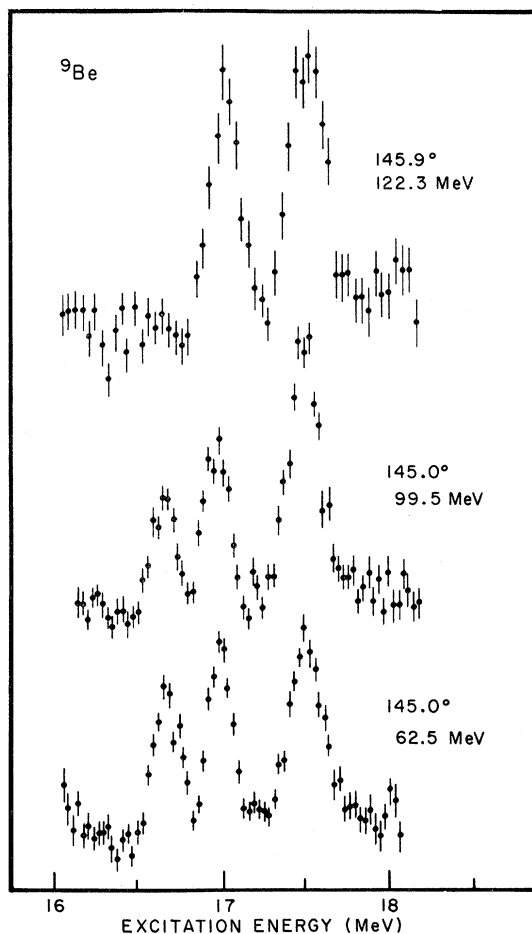


FIG. 2. Spectra of electrons inelastically scattered from  $^9\text{Be}$  near 17 MeV excitation. The three peaks correspond to levels at 16.63, 16.96, and 17.48 MeV excitation, as determined by this experiment. The 17.48-MeV peak is broader than the others, reflecting the natural width of this state ( $\sim 50$  keV) (Ref. 3). The ordinate scales for the three spectra are not identical.

parameter  $N$  is the scale factor which depends on target thickness, etc., and  $Q$  corresponds to the spectroscopic quadrupole moment. The rms radius is determined by  $\alpha$  and  $b$ .

The errors associated with the elastic data are a combination of the errors based on the counting statistics, typically  $\sim 1\%$ , and errors which may be described as "deviations" not associated with counting statistics. These "deviations" include an accumulation of instrumental effects; for example, micrometer measurements on the beryllium target revealed local thickness variations of about 3%. A series of least-squares fits of the modified areas, uncorrected for Coulomb distortion, were made to four-parameter functions similar to those given in Eq. (1). Only the statistical errors were used in the fitting procedure. That fit which gave the lowest  $\chi^2$  was chosen as providing a measure of the self-consistency of the data. The statistical errors were then scaled by  $(\chi^2/\text{degree of freedom})^{1/2}$ , which corresponded to a scale factor of about 2.

#### Inelastic Scattering

The cross section for the electroexcitation of a discrete level can be written, in the first Born

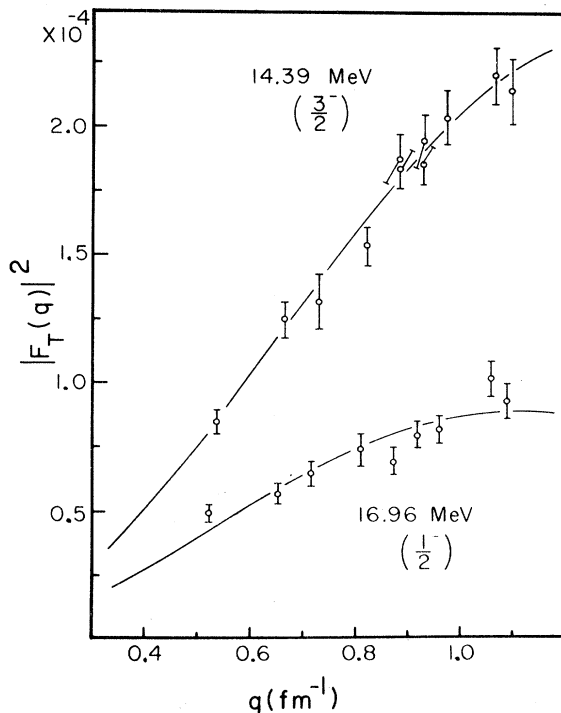


FIG. 3. Transverse form factors for the  $T = \frac{3}{2}$  levels in  ${}^9\text{Be}$ . The solid lines represent generalized Helm model fits for  $M1$  transitions.

approximation

$$\frac{d\sigma}{d\Omega} = \sigma_M \left\{ \frac{q_\mu^4}{q^4} |F_L(q)|^2 + \left[ \frac{q_\mu^2}{2q^2} + \tan^2(\theta/2) \right] |F_T(q)|^2 \right\}, \quad (2)$$

where

$$\sigma_M = \left( \frac{Z\alpha}{2E_0} \right)^2 \frac{\cos^2(\theta/2)}{\sin^4(\theta/2)} \left[ 1 + \frac{2E_0}{M} \sin^2(\theta/2) \right]^{-1} \quad (3)$$

is the Mott cross section. Here  $F_L(q)$  and  $F_T(q)$  are the longitudinal and transverse form factors for the transition, and  $q^2$ ,  $q_\mu^2$  are the squares of the three- and four-momentum transfers, respectively. Previous angular-distribution measurements at constant  $q$  at this facility<sup>8</sup> and elsewhere<sup>5</sup> have shown that the electroexcitation cross sections for the levels in the 14- to 18-MeV excitation region have at most very small longitudinal contributions. Consequently, in the analysis we have neglected the longitudinal components; i.e. the form factors were considered to be completely transverse.

The inelastic spectra were fitted by a nonlinear least-squares program which synthesized the observed spectra in terms of a series of analytic peak shapes superimposed on a smooth polynomial background function. The analytic shapes were integrated to specified energy cutoffs (two or three peak widths below the maxima), and the asso-

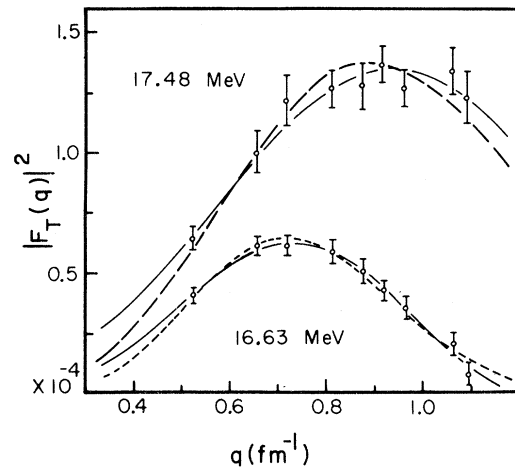


FIG. 4. Transverse form factors for the 16.63- and 17.48-MeV levels. The solid curve through the 16.63-MeV data represents the generalized Helm model fit for an  $M1$  transition, and the short-dashed curve is the  $E2$  (spin-flip) fit, which is slightly poorer. The  $E1$  and  $M2$  fits to the 16.63-MeV data are nearly indistinguishable from the solid curve. The solid curve through the 17.48-MeV data represents an  $M1$  fit, while the long-dashed curve represents  $E1$  and  $M2$  fits, which are nearly identical.

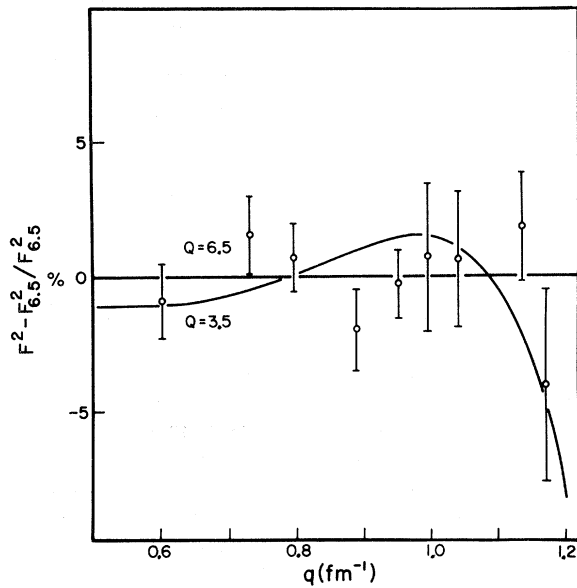


FIG. 5. Comparison of the elastic scattering data, corrected for Coulomb distortion, with the least-squares fit to Eq. (1), using  $Q = 6.5 \text{ fm}^2$ . The form factor with this  $Q$  is referred to as  $F_{6.5}^2$ . Also indicated is the comparison of the  $Q = 3.5\text{-fm}^2$  fit with  $F_{6.5}^2$ .

ciated errors were evaluated from the total error matrix. Inelastic form factors  $|F_T(q)|^2$  were obtained by comparing the inelastic to elastic peak areas, using the elastic form factor to provide the necessary calibration.

The transverse form factors for the  $\frac{3}{2}^-$  (14.39-MeV) and  $\frac{1}{2}^-$  (16.96-MeV)  $T = \frac{3}{2}$  levels are shown in Fig. 3. The results for the 16.63- and 17.48-MeV levels are displayed in Fig. 4. The error bars in these figures were generated from a linear combination of the errors evaluated in the shape fitting of the inelastic spectra, and the er-

ror associated with the elastic form factor. This procedure was adopted to give a reliable upper bound to the errors, some components of which may not be statistical in origin.

Numerical values of the transverse inelastic form factors are presented in Table I.

#### IV. RESULTS AND DISCUSSION

##### Elastic Scattering

The rms radius, the quadrupole moment  $Q$ , and the oscillator parameter  $b$  as determined in the present experiment are

$$\langle r^2 \rangle^{1/2} = 2.46 \pm 0.11 \text{ fm},$$

$$Q = 6.5 \begin{smallmatrix} +0.9 \\ -0.6 \end{smallmatrix} \text{ fm}^2,^9$$

$$b = 1.5 \begin{smallmatrix} +0.3 \\ -0.2 \end{smallmatrix} \text{ fm}.$$

This  $\langle r^2 \rangle^{1/2}$  is consistent with previous measurements obtained at lower momentum transfers:

$$\langle r^2 \rangle^{1/2} = 2.519 \pm 0.012 \text{ fm},^{10}$$

$$Q = 3.2 \pm 1.2 \text{ fm}^2,$$

$$\langle r^2 \rangle^{1/2} = 2.46 \pm 0.09 \text{ fm}.^{11}$$

However, the present value for  $Q$ , although model-dependent, is much larger than that obtained in the low- $q$  measurements. A fit of Eq. (1) to the data, with  $Q = 3.5 \text{ fm}^2$ , yields  $\langle r^2 \rangle^{1/2} = 2.51 \text{ fm}$  which is close to the rms radius found by Jansen, Peerderman, and De Vries,<sup>10</sup> but the  $\chi^2$  of the fit doubles to  $\chi^2 \approx 12$  for 6 degrees of freedom. In Fig. 5 the data and the fit for  $Q = 3.5 \text{ fm}^2$  are compared with the fit for  $Q = 6.5 \text{ fm}^2$ .

Bouten *et al.*<sup>12</sup> have analyzed the elastic scattering data of Meyer-Berkhout *et al.*, Nguyen-Ngoc *et al.*, and Bernheim *et al.* in terms of wave func-

TABLE I. Transverse form factors for levels in  $^9\text{Be}$  as measured in the present experiment.

$q$ ( $\text{fm}^{-1}$ )	$E_x$ (MeV)		$q$ ( $\text{fm}^{-1}$ )	$ F_T(q) ^2 \times 10^5$	$ F_T(q) ^2 \times 10^5$	17.48
	14.39	16.63				
	$ F_T(q) ^2 \times 10^5$					
0.53	$8.51 \pm 0.5$	0.52	$4.06 \pm 0.28$	$4.93 \pm 0.32$	$6.40 \pm 0.47$	
0.66	$12.5 \pm 0.7$	0.65	$6.12 \pm 0.40$	$5.71 \pm 0.42$	$9.99 \pm 0.86$	
0.73	$13.2 \pm 1.1$	0.72	$6.12 \pm 0.41$	$6.49 \pm 0.45$	$12.2 \pm 1.1$	
0.82	$15.4 \pm 0.8$	0.81	$5.84 \pm 0.48$	$7.42 \pm 0.64$	$12.7 \pm 0.8$	
0.89	$18.4 \pm 0.8$	0.87	$5.04 \pm 0.49$	$6.97 \pm 0.53$	$12.8 \pm 1.0$	
0.89	$18.8 \pm 1.0$	0.92	$4.26 \pm 0.42$	$8.00 \pm 0.50$	$13.7 \pm 0.8$	
0.93	$18.6 \pm 0.8$	0.96	$3.50 \pm 0.43$	$8.23 \pm 0.53$	$12.7 \pm 0.8$	
0.93	$19.5 \pm 1.1$	1.06	$2.03 \pm 0.48$	$10.22 \pm 0.68$	$13.4 \pm 1.0$	
0.97	$20.4 \pm 0.9$	1.09	$0.78 \pm 0.46$	$9.32 \pm 0.69$	$12.3 \pm 1.1$	
1.07	$22.1 \pm 1.1$					
1.10	$21.5 \pm 1.3$					

tions derived from a projected Hartree-Fock calculation. Their results suggest a quadrupole moment between 5.5 and 6 fm<sup>2</sup>. The quadrupole moment has also been deduced from a hyperfine-structure measurement, and with a Sternheimer shielding correction applied, a value  $Q = 5.3 \pm 0.3$  fm<sup>2</sup> is obtained.<sup>13</sup>

#### Inelastic Scattering

#### Radiative Widths

The possible transition multipolarities and corresponding radiative widths of the excited states have been determined by least-squares fitting the experimental form factors to the generalized Helm model of Rosen, Raphael, and Überall<sup>14</sup> using the first Born approximation. According to this phenomenological description, the transition magnetization and current densities are Gaussian functions, described by a width parameter  $g$ , centered at a radius  $R$  in the nucleus. The reduced matrix elements for  $E\lambda$  (transverse) and  $M\lambda$  transitions are given by

$$\begin{aligned} \langle J' \| T_{\lambda}^e(q) \| J_0 \rangle / (2J_0 + 1)^{1/2} \\ = c_1^e \left( \frac{\lambda + 1}{\lambda} \right)^{1/2} \frac{\omega}{q} h(q) j_{\lambda}(qR) + c_2^e \frac{q}{2M} \bar{h}(q) j_{\lambda}(q\bar{R}), \end{aligned} \quad (4)$$

$$\begin{aligned} \langle J' \| T_{\lambda}^m(q) \| J_0 \rangle / (2J_0 + 1)^{1/2} \\ = -\frac{q}{2M} \bar{h}(q) \left[ c_1^m \left( \frac{\lambda}{2\lambda + 1} \right)^{1/2} j_{\lambda+1}(q\bar{R}) \right. \\ \left. + c_2^m \left( \frac{\lambda + 1}{2\lambda + 1} \right)^{1/2} j_{\lambda-1}(q\bar{R}) \right], \end{aligned} \quad (5)$$

where

$$h(q) = e^{-g^2 q^2 / 2},$$

$$\bar{h}(q) = e^{-\bar{g}^2 q^2 / 2},$$

and  $M$  is the nucleon mass,  $J_0$  and  $J'$  are, respectively, the ground- and excited-state spins. The parameters  $c_1$ ,  $c_2$ ,  $R$ ,  $\bar{R}$ ,  $g$ , and  $\bar{g}$  are to be determined from the data for a given value of  $\lambda$ . For so-called pure spin-flip  $E\lambda$  transitions,  $c_1^e = 0$  since the matrix element has no longitudinal counterpart. The radiative widths predicted by the generalized Helm model are

$$\begin{aligned} \Gamma_{\gamma_0}^e = 8\pi\alpha \frac{\lambda + 1}{\lambda [(2\lambda + 1)!!]^2} \omega^{2\lambda + 1} \\ \times R^{2\lambda} \frac{2J_0 + 1}{2J' + 1} (c_1^e)^2, \end{aligned} \quad (6)$$

$$\begin{aligned} \Gamma_{\gamma_0}^m = 8\pi\alpha \frac{\lambda + 1}{\lambda [(2\lambda + 1)!!]^2} \omega^{2\lambda + 1} \bar{R}^{2\lambda} (2\lambda + 1) \\ \times \left( \frac{1}{2M\bar{R}} \right)^2 \frac{2J_0 + 1}{2J' + 1} (c_2^m)^2. \end{aligned} \quad (7)$$

Only  $M1$  transitions give a satisfactory description of the  $T = \frac{3}{2}$  (14.39- and 16.96-MeV) data in the Helm model. This confirms the negative-parity assignments for these levels. The  $M1$  Helm-model form factors for these levels are shown in Fig. 3.

The 16.63-MeV level was assigned a positive parity ( $M2$  or spin-flip  $E1$  transition) by Clerc *et al.*<sup>5</sup> based on the behavior of the form factor at low momentum transfers. For this state we find equally good fits for  $M1$ ,  $M2$ , and spin-flip  $E1$  transitions, and a slightly poorer fit for  $E2$ . The results are shown in Fig. 4.

The peak we observe at 17.48 MeV excitation consists of an unresolved doublet whose components lie at 17.28 and 17.48 MeV.<sup>3</sup> In all our spectra, the peak shape for this doublet was centered close to 17.48 MeV excitation, which suggests that the 17.48-MeV level has the dominant strength. A recent angular-distribution study of the  ${}^7\text{Li}(d, \alpha){}^5\text{He}$  reaction by Friedland and Venter<sup>15</sup> indicates  $J^{\pi} = \frac{3}{2}^+$ ,  $\frac{5}{2}^+$ , or  $\frac{7}{2}^+$  for the 17.28-MeV level, and  $\frac{1}{2}^-$  or  $\frac{3}{2}^-$  for the 17.48-MeV level. However, Clerc *et al.*<sup>5</sup> conclude that the 17.48-MeV state has positive parity ( $M2$  transition or spin-flip  $E1$ ).

The transition multipolarity which yields the

TABLE II. Summary of ground-state radiation widths from the present experiment and other work. The statistical factor  $g$  is defined by  $g = (2J_0 + 1)/(2J + 1)$ , with  $J_0 = \frac{3}{2}$ .  $\Gamma_w$  is the single-particle Weisskopf unit.

$E_x$ (MeV)	$J^{\pi}$		$\Gamma_{\gamma_0}$ (eV)		$\Gamma_{\gamma_0}/\Gamma_w$			
			Experiment	Theory <sup>a</sup>				
14.39	$\frac{3}{2}^-$	(M1)	$6.2 \pm 0.6$ <sup>b</sup>	5.3				
			$8.1 \pm 0.8$ <sup>c</sup>					
			$6.7 \pm 1.4$ <sup>d</sup>					
			$6.9 \pm 0.5$ <sup>e</sup>					
				0.11				
16.96	$\frac{1}{2}^-$	(M1)	$11.5 \pm 1.4$ <sup>b</sup>	15	0.11			
			$8.6 \pm 0.9$ <sup>c</sup>					
16.63	$\leq \frac{3}{2}^-$	(M1)	$(2.0 \pm 0.5) g$ <sup>b</sup>	2.4 <sup>f</sup>	0.021g			
			$\leq \frac{1}{2}^+$			(M2) $(0.26 \pm 0.02) g$ <sup>b</sup>	3.2g	
			(M2) $(0.32 \pm 0.08) g$ <sup>c</sup>					
(17.28)	$\leq \frac{3}{2}^-$	(M1)	$(7.3 \pm 1.3) g$ <sup>b</sup>	0.92 <sup>g</sup>	0.065g			
			(17.48)			$\leq \frac{1}{2}^+$	(M2) $(0.40 \pm 0.03) g$ <sup>b</sup>	3.8g

<sup>a</sup> Reference 1.

<sup>b</sup> Present results.

<sup>c</sup> Reference 5.

<sup>d</sup> Reference 8.

<sup>e</sup> Weighted average.

<sup>f</sup>  $JT = \frac{3}{2} \frac{1}{2}$  (15.8 MeV).

<sup>g</sup>  $\frac{5}{2} \frac{1}{2}$  (17.6 MeV) +  $\frac{3}{2} \frac{1}{2}$  (17.9 MeV).

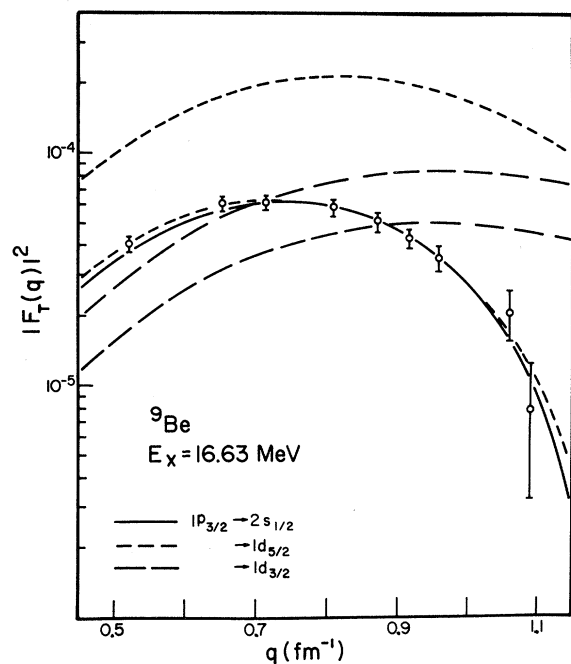


FIG. 6. Shell-model  $M2$  form factors for a neutron transition from the  $1p_{3/2}$  to the  $2s-1d$  shell, compared with the form factor for the 16.63-MeV level. The oscillator parameter  $b_0$  and the neutron effective charge  $e_n$  have been varied by the method of least squares to give the best fit to the data. The higher-lying member of each pair of form factors has been computed with  $e_n = 0$ , but with the same  $b_0$  as the lower-lying member. The  $1p_{3/2} \rightarrow 2s_{1/2}$  form factor is independent of  $e_n$ .

best fit of the generalized Helm model to the present data on the 17.48-MeV level is  $M1$  (Fig. 4). Although the  $M2$  and spin-flip  $E1$  fits are also satisfactory, all other multipoles can clearly be rejected. An  $M1$  assignment implies  $J^\pi \leq \frac{5}{2}^-$  for this level, while an  $M2$  transition would give  $J^\pi \leq \frac{7}{2}^+$ . While the latter is in agreement with the results of Clerc *et al.*, none of these assignments are consistent with the conclusions of Friedland and Venter.

Table II summarizes the radiative widths derived from the  $M1$  and  $M2$  Helm-model fits to the form factors. Included for comparison are the results of previous measurements,<sup>5,8</sup> and the theoretical values from the intermediate-coupling calculation of Barker.<sup>1</sup> Reasonable agreement is seen to exist between theory and experiment for the  $T = \frac{3}{2}$  levels. Barker's results do not include any levels which could be immediately identified as the 16.63-MeV excitation, however a level is predicted at 15.8 MeV ( $\frac{3}{2}^-$ ,  $T = \frac{1}{2}$ ) whose  $M1$  radiative width is close to that of the 16.63-MeV level. This tentative identification has been included in Table II. As for the 17.48-MeV level,  $T = \frac{1}{2}$  levels are predicted at

17.6 ( $\frac{5}{2}^-$ ) and 17.9 MeV ( $\frac{3}{2}^-$ ), but the sum of the theoretical ground-state  $M1$  radiative widths is much smaller than the present experimental value for the 17.48-MeV peak.

Also presented in Table II are the ratios of the radiative widths to the single-particle Weisskopf estimates.

#### Total Width of 14.39-MeV Level

The ground states of  ${}^9\text{C}$  and  ${}^9\text{Li}$ , together with the  $T = \frac{3}{2}$  levels at 14.39 MeV in  ${}^9\text{Be}$  and 14.66 MeV in  ${}^9\text{B}$  form an isospin quartet which has recently become the subject of investigation in an attempt to gain information on isospin impurities in light nuclei.<sup>16,17</sup> The 14.39-MeV level in  ${}^9\text{Be}$  is bound to isospin-conserving particle decay, therefore  $\Gamma_{\text{tot}}$  is a measure of the isospin impurities in this level. Using the weighted mean ratio  $\Gamma_{\gamma_0}/\Gamma_{\text{tot}} = 0.022 \pm 0.003$  from the results of Refs. 16 and 18, together with the average radiative width  $\Gamma_{\gamma_0}(M1)$  from Table II, one obtains  $\Gamma_{\text{tot}} = 0.31 \pm 0.05$  keV. This is somewhat smaller than previously reported values of 0.5 keV<sup>16</sup> and 0.8 keV.<sup>3</sup>

Adloff *et al.*<sup>17</sup> used  $\Gamma_{\gamma_0}(M1) = 10.5 \pm 1.5$  eV in evaluating the partial-neutron and -proton widths of the  ${}^9\text{Be}$  and  ${}^9\text{B}$  analog states. With the present value  $\Gamma_{\gamma_0} = 6.9 \pm 0.5$  eV, the partial widths found by these authors should be reduced by the factor 6.9/10.5.

#### 16.63-MeV Level

The form factor for this level is slightly unusual in that it has a maximum at a relatively low momentum transfer, about  $0.7 \text{ fm}^{-1}$ . This behavior has been seen in a few other light nuclei, for example the  $M1$  transition to the 3.56-MeV ( $0^+$ ,  $T=1$ ) state in  ${}^6\text{Li}$ .<sup>19</sup>

The model analysis of the 16.63-MeV state is complicated by the ambiguity in  $J^\pi$ . If the parity is negative, the only candidate in Barker's calculation<sup>1</sup> is the predicted level at 15.8 MeV ( $\frac{3}{2}^-$ ,  $T = \frac{1}{2}$ ), which has an  $M1$  radiative width comparable to that of the 16.63-MeV transition (Table II). Form factors for this and the other states, using Barker's wave functions, have not yet been calculated.

On the other hand, if the parity is positive, the simplest model is the promotion of a  $1p$  nucleon to the  $2s-1d$  shell. As a test of this model, form factors have been calculated in the framework of the spherical and deformed (Nilsson) harmonic oscillator, in the first Born approximation.

*Shell Model.* For the calculation based on a simple spherical shell model, the neutron is raised from the  $1p_{3/2}$  to the  $1d_{5/2}$ ,  $2s_{1/2}$ , or  $1d_{3/2}$  shells. The assumption is made that the  ${}^8\text{Be}$  core remains an inert spectator, so the excited state necessarily has  $T = \frac{1}{2}$  in this description. The single-particle-transition matrix elements follow

from the expressions given by de Forest and Walecka,<sup>20</sup> and for  $M2$  transitions one obtains for

$1p_{3/2} \rightarrow 2s_{1/2}$ :

$$\langle n'l'j' \| T_2^{\text{mag}}(q) \| nlj \rangle = i(0.461\mu_n/Mb_0)y(1-y)e^{-y}; \quad (8)$$

for  $1p_{3/2} \rightarrow 1d_{3/2}$ :

$$\langle n'l'j' \| T_2^{\text{mag}}(q) \| nlj \rangle = i(0.291/Mb_0)(\mu_n - e_n)ye^{-y}; \quad (9)$$

for  $1p_{3/2} \rightarrow 1d_{5/2}$ :

$$\langle n'l'j' \| T_2^{\text{mag}}(q) \| nlj \rangle = i(0.668/Mb_0)[(1 - 0.476y)\mu_n + 2e_n/3]ye^{-y}, \quad (10)$$

where  $y = (qb_0/2)^2$ ,  $b_0$  is the harmonic-oscillator parameter,  $\mu_n = -1.91$ , and  $e_n$  is the "effective charge" of the neutron. The form factor is given by

$$F_T^2(q) = \frac{4\pi}{Z^2} \frac{|\langle n'l'j' \| T_\lambda(q) \| nlj \rangle|^2}{2J_0 + 1} e^{2y/A} f^2(q), \quad (11)$$

where  $f(q)$  is the nucleon form factor, the exponential factor is the usual center-of-mass correction term,<sup>20</sup> and  $A$  is the mass number.

The above expressions contain two variables,  $b_0$  and  $e_n$  (except for the  $1p_{3/2} \rightarrow 2s_{1/2}$  transition, which is independent of  $e_n$ ). These parameters were varied to give a least-squares fit to the data, and the results are shown in Fig. 6. The parameters which give the best  $M2$  fits are:

$$1p_{3/2} \rightarrow 2s_{1/2}: \quad b_0 = 1.65 \text{ fm};$$

$$1p_{3/2} \rightarrow 1d_{5/2}: \quad b_0 = 1.89 \text{ fm}, \quad e_n = 0.99;$$

$$1p_{3/2} \rightarrow 1d_{3/2}: \quad b_0 \geq 2.1 \text{ fm}, \quad e_n = -0.45.$$

Included in Fig. 6 are the form factors calculated with  $e_n = 0$ .

The data are seen to be fairly well described by an  $M2$  neutron transition to the  $2s_{1/2}$  or  $1d_{5/2}$  shells. The values for  $b_0$  are larger than the parameter  $b$  extracted from the elastic scattering data. This is not surprising, since the 16.63-MeV level lies well within the neutron continuum, so the radius of a  $2s$ - $1d$ -shell neutron would be larger than that predicted using the infinite harmonic-oscillator potential which describes the ground-state properties.

Form factors for  $E1$  transitions to the  $2s_{1/2}$ ,  $1d_{3/2}$ , and  $1d_{5/2}$  shells have also been calculated in the single-particle model. The apparent absence of a longitudinal component in the experimental form factor implies a very small, or zero, neutron  $E1$  effective charge. Assuming  $e_n(E1) = 0$ , the  $E1$  matrix elements are:

$1p_{3/2} \rightarrow 2s_{1/2}$ :

$$\langle n'l'j' \| T_1^{\text{el}}(q) \| nlj \rangle = (0.266\mu_n/Mb_0)y(y-1)e^{-y}; \quad (12)$$

$1p_{3/2} \rightarrow 1d_{3/2}$ :

$$\langle n'l'j' \| T_1^{\text{el}}(q) \| nlj \rangle = (0.752\mu_n/Mb_0)y(1-0.4y)e^{-y}; \quad (13)$$

$1p_{3/2} \rightarrow 1d_{5/2}$ :

$$\langle n'l'j' \| T_1^{\text{el}}(q) \| nlj \rangle = (0.564\mu_n/Mb_0)y(1-0.4y)e^{-y}. \quad (14)$$

The  $E1$  form factors do not agree with the data unless they are scaled by over-all multiplicative factors. Also, the  $1d$ -shell transition matrix elements require very large  $b_0$  to put the maximum at the observed position. However, the possibility of  $E1$ - $M2$  mixing cannot be excluded. Unfortunately, the electron-scattering data do not provide a sensitive measure of the mixing ratios.

*Strong-Coupling Model.* It has been suggested that the  ${}^9\text{Be}$  ground state ( $J^\pi = \frac{3}{2}^-$ ), the 2.43- ( $\frac{5}{2}^-$ ), and 6.66-MeV ( $\frac{7}{2}^-$ ) states are members of a  $K = \frac{3}{2}$  rotational band. Furthermore, the first and second excited states of  ${}^9\text{Be}$  are broad resonances which approximately lie on a rotational sequence. Therefore, the ground state of  ${}^9\text{Be}$  could be described as a neutron bound to an axially deformed  ${}^8\text{Be}$  core. If the component of the total nuclear angular momentum  $J$  along the intrinsic-symmetry axis is denoted by  $K$ , and the projection of the angular momentum of the valence neutron along the same axis is  $\Omega$ , then, for  $\Omega = K$ , the



nuclear wave function is<sup>21</sup>

$$|JMK\rangle = \left(\frac{2J+1}{16\pi^2}\right)^{1/2} [D_{MK}^J(\hat{r})\chi_K + (-1)^{J+K+\Omega} D_{M-K}^J(\hat{r}) \sum_j (-1)^j c_{jK} \chi_{j-K}], \quad (15)$$

where  $\chi_K = \sum_j c_{jK} \chi_{jK}$  is an expansion of the single-particle orbital in terms of a set of undeformed-potential orbitals  $\chi_{jK}$  (shell-model functions, for example).

In the strong-coupling model, the 16.63-MeV transition might be interpreted as a transition of the valence neutron from the  $\Omega = \frac{3}{2}^- [101]$  Nilsson orbital ( $1p_{3/2}$  shell in the limit of zero deformation) to one of the six Nilsson orbitals which degenerate into the  $1d_{5/2}$ ,  $2s_{1/2}$ , and  $1d_{3/2}$  shells at zero deformation. The transition matrix element in this model can be shown to be

$$\begin{aligned} \langle J'K' \| T_\lambda(q) \| J_0K_0 \rangle = & [(2J_0+1)(2J'+1)]^{1/2} \sum_{jj'} c_{j'K'} c_{jK_0} \langle j' \| T_\lambda(q) \| j \rangle \\ & \times \left[ (-1)^{J'-j'} \begin{pmatrix} J' & \lambda & J_0 \\ -K' & \mu & K_0 \end{pmatrix} \begin{pmatrix} j' & \lambda & j \\ -K' & \mu & K_0 \end{pmatrix}_{\mu=K'-K_0} + \begin{pmatrix} J' & \lambda & J_0 \\ K' & \mu & K_0 \end{pmatrix} \begin{pmatrix} j' & \lambda & j \\ K' & \mu & K_0 \end{pmatrix}_{\mu=-K'+K_0} \right]. \end{aligned} \quad (16)$$

If the contribution of the core is neglected,  $\langle j' \| T_\lambda(q) \| j \rangle$  is simply the  $M2$  and  $E1$  single-particle matrix elements, given by Eqs. (8) to (10), and (12) to (14), respectively.

The matrix elements contain the free parameters  $b_0$ ,  $e_n$ , and the deformation parameter  $\beta$ . A brief search was made, varying  $b_0$  and  $e_n$ , for the best fit to the 16.63-MeV form factor ( $e_n$  is assumed to be zero for the  $E1$  transitions, as mentioned above). The deformation was fixed at  $\beta=0.3$  (prolate deformation), and the  $c_{jK}$  coefficients tabulated by Davidson<sup>22</sup> were used. Of the six Nilsson orbitals which were tried in the final-state function, acceptable  $M2$  fits were obtained only for the  $\frac{1}{2}^+ [220]$  orbital, with  $J' = \frac{1}{2}$  and  $\frac{5}{2}$ . The corresponding values of the oscillator constant and neutron effective charge are

$$J' = \frac{1}{2}, \quad b_0 = 1.96 \text{ fm}, \quad e_n = -0.5,$$

$$J' = \frac{5}{2}, \quad b_0 = 2.00 \text{ fm}, \quad e_n = -0.5.$$

The  $M2$  form factors for a neutron transition between the  $\frac{3}{2}^- [101]$  and  $\frac{1}{2}^+ [220]$  Nilsson orbitals are compared with the experimental results in Fig. 7. The only reasonable  $E1$  fit is for the  $\frac{3}{2}^- [101] \rightarrow \frac{1}{2}^+ [211]$  transition, for which one obtains  $J' = \frac{1}{2}$ ,  $b_0 = 2.06 \text{ fm}$ , and is also included in Fig. 7.

In fitting the undeformed- and deformed-shell model  $M2$  form factors to the data, the effective charge  $e_n$  of the neutron has been treated as a variable, while the magnetic moment was fixed at the usual value. The reduced matrix elements in Eq. (16) were evaluated ignoring the contribution from the core excitation for simplicity. However, a more detailed calculation would show that the core contribution could be included by considering  $e_n$  and the magnetic moment of the neutron to be functions of  $q$ . This can be seen roughly as follows.

The magnetic-moment operator  $\vec{\mu}_c(\vec{r})$  of the core is given by  $g_c [\rho(\vec{r}) \vec{L}]_{\text{sym}}$ , where  $\vec{L}$  is the core angular momentum and  $\vec{\mu}_c(\vec{r})$  has been given the same spatial distribution as the charge density  $\rho(\vec{r})$ . Replacing  $\vec{L}$  by  $\vec{J} - \vec{j}$ , where  $\vec{j}$  is the neutron angular momentum (neither  $\vec{L}$  nor  $\vec{j}$  are conserved), one sees that the core matrix element contributes a term in  $\vec{j}$  which in effect modifies the neutron magnetic-moment operator  $\vec{\mu}_n(\vec{r}) = (g_s \vec{s} + g_l \vec{l}) \delta(\vec{r} - \vec{r}_i)$ . The net result is to replace  $g_l$ , which depends on  $e_n$ , and  $g_s$ , which depends on the free magnetic moment, by functions of  $q$  which depend on the details of the core-transition charge density.

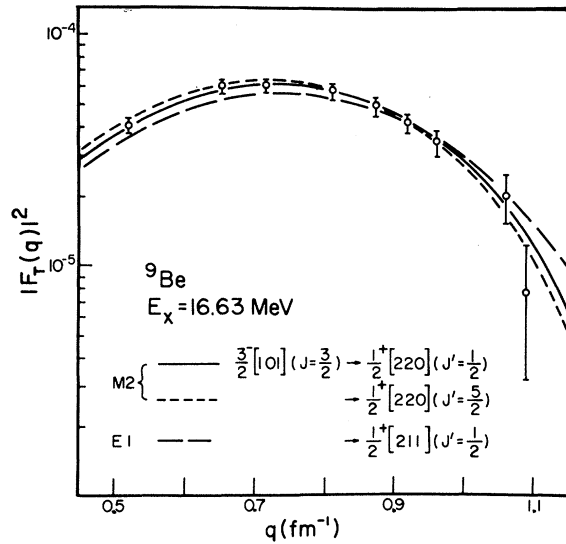


FIG. 7. Strong-coupling model  $M2$  and  $E1$  form factors for the promotion of a neutron from the  $K = \frac{3}{2}^- [101]$  orbital to the  $K' = \frac{1}{2}^+ [220]$  and  $\frac{1}{2}^+ [211]$  orbitals. The deformation parameter is  $\beta=0.3$ . The effective charges of the neutron are  $e_n(M2) = -0.5$ ,  $e_n(E1) = 0.0$ .

## V. CONCLUSION

The  ${}^9\text{Be}$  elastic scattering data have been interpreted within the framework of a charge distribution generated by protons moving in the  $1s$  and  $1p$  shells of an undeformed harmonic-oscillator potential. However, the  $1p$ -shell contribution to the  $E0$  form factor [the  $\alpha$  term in Eq. (1)] was not constrained to the shell-model value. The electric quadrupole moment in this model arises from the  $p$ -shell protons and was treated as a variable-scale parameter.

The rms radius obtained from the present experiment is consistent with other electron-scattering results, but the quadrupole moment is larger than found from previous measurements. Whether this disagreement is a consequence of the particular model used has not been explored. The experimental values for the quadrupole moment of  ${}^9\text{Be}$  range from  $2\text{ fm}^2$  to more than  $6\text{ fm}^2$ , and the theoretical predictions vary as much.<sup>12</sup> An absolute measurement of the  ${}^9\text{Be}$  elastic form factor is currently in progress at this facility, with a greater range of momentum transfer than reported here, in an attempt to obtain a more accurate value for  $Q$ .

The intermediate-coupling calculation of Barker suggests three  $T = \frac{3}{2}$  levels below 18 MeV excitation in  ${}^9\text{Be}$ . The lowest of these is the state at 14.39 MeV ( $\frac{3}{2}^-$ ), for which the theoretical and experimental ground-state radiative widths are in reasonable agreement (Table II). The other two levels should be near 17 MeV excitation, with  $J^\pi = \frac{1}{2}^-$  and  $\frac{5}{2}^-$ . The predicted radiative width of the  $\frac{1}{2}^-$  level is in satisfactory agreement with the experimental value for the 16.96-MeV level, but the predicted width for the  $\frac{5}{2}^-$  state is much smaller, about 0.003 eV, and so would not be seen in the present experiment. Thus, there is little doubt that the 16.96 MeV excitation is the  $TJ^\pi = \frac{3}{2} \frac{1}{2}^-$  state.

A fourth  $T = \frac{3}{2}$  ( $\frac{3}{2}^-$ ) level is predicted by the intermediate-coupling calculation to lie near 18.7 MeV. The theoretical ground-state radiative width is about 2.5 eV, so it should be observable by inelastic electron scattering. A broad bump does indeed appear in the spectra around 18.6 MeV excitation (see Fig. 1), which may be the same broad peak seen in  ${}^7\text{Li}(d, p)$ ,  ${}^7\text{Li}(d, \alpha)$ , and  ${}^6\text{Li}(t, \alpha)$  reactions.<sup>3</sup> Whether or not these reactions proceed via isospin impurities in a predominantly  $T = \frac{3}{2}$  state is not known.

Let us now consider the 16.63-MeV level. The Helm-model analysis is consistent with  $M1$ ,  $M2$ , spin-flip  $E1$ , and possibly  $E2$  transitions. The  $E2$  fit can probably be rejected since it requires  $\bar{g} \geq 2$ , about twice the usual value

associated with a transition density. Calculations of  $E1$  and  $M2$  form factors, for the promotion of the valence neutron to the  $2s-1d$  shell of an undeformed harmonic oscillator, were compared with the data. The  $M2$ ,  $1p_{3/2} \rightarrow 2s_{1/2}$  form factor, which contains one free parameter ( $b_0$ ), gives a good description of the data with  $b_0 = 1.65\text{ fm}$ . This  $b_0$  is larger than that obtained from the elastic scattering data, and corresponds to an oscillator spacing  $\hbar\omega_0 = 15.3\text{ MeV}$ . The  $M2$ ,  $1p_{3/2} \rightarrow 1d_{5/2}$  form factor also fits the data, but  $b_0$  is somewhat larger, and a second parameter, the neutron  $M2$  effective charge must have a value near unity. The corresponding  $E1$  form factors do not agree with the data unless they are re-normalized.

Although the simple harmonic-oscillator results are encouraging, they are probably not realistic, since  ${}^9\text{Be}$  is known to be a deformed nucleus. Consequently, a strong-coupling model (with inert core) was tried in which the neutron is promoted by  $M2$  or spin-flip  $E1$  transitions to one of the six Nilsson orbitals based on the  $2s-1d$  shell. Only the  $M2$  and  $E1$  form factors calculated, respectively, with the  $\frac{1}{2}^+ [220]$  and  $\frac{1}{2}^+ [211]$  orbitals are consistent with the 16.63-MeV level data and both required  $b_0 \approx 2\text{ fm}$ . Since  $b_0$  is an effective average of the  $1p$ - and  $2s-1d$ -shell oscillator parameters, the actual  $b_0$  value for the above excited-state orbitals may be larger than this. The separation between these orbitals and the ground-state valence orbital ( $\frac{3}{2}^- [101]$ ), at a deformation  $\beta = 0.3$  and  $b_0 = 2\text{ fm}$ , is only about 5–9 MeV, while the observed excitation energy is 16.6 MeV. Therefore, none of the orbitals which were considered seem to give a consistent description of the experimental data and excitation energy of this state.

The preceding discussion assumes a positive-parity assignment for the 16.63-MeV level. On the other hand, intermediate coupling within the  $1s^4 1p^5$  configuration<sup>1</sup> yields a state at 15.8 MeV ( $\frac{3}{2}^-$ ,  $T = \frac{1}{2}$ ) with the  $M1$  radiative width comparable to that found for the 16.63-MeV level. The form factor has not been calculated, but the tentative identification is supported by the observation that no narrow level of corresponding strength is seen near 15.8 MeV. A weak peak appears in the spectra at 15.93 MeV, but the radiative width is probably less than 2 eV.

The generalized Helm-model analysis is not sufficient to assign a parity to the 17.48-MeV level, since  $M1$  and  $M2$  fits are both satisfactory. However, if once again we use Barker's calculation as a guide, the prediction of no strong negative levels in this region would suggest a positive parity for the observed peak, and therefore  $J^\pi \leq \frac{7}{2}^+$ .

## ACKNOWLEDGMENT

The authors wish to thank Dr. E. Tomusiak for helpful discussions.

\*Work supported by the Atomic Energy Control Board of Canada.

†Present address: Physics Department, Stellenbosch University, Stellenbosch, C. P., South Africa.

<sup>1</sup>F. C. Barker, Nucl. Phys. 83, 418 (1966).

<sup>2</sup>H. G. Clerc, K. J. Wetzal, and E. Spamer, Nucl. Phys. A120, 441 (1968).

<sup>3</sup>T. Lauritsen and F. Ajzenberg-Selove, Nucl. Phys. 78, 1 (1966).

<sup>4</sup>C. L. Cocke, Nucl. Phys. A110, 321 (1968).

<sup>5</sup>H. G. Clerc, K. J. Wetzal, and E. Spamer, Phys. Letters 20, 667 (1966); H. Theissen, Institute for Nuclear Physics, Darmstadt Report, 1972 (unpublished).

<sup>6</sup>H. S. Caplan, I. P. Auer, J. H. Hough, J. C. Bergstrom, and F. J. Kline, to be published.

<sup>7</sup>See, for example, J. C. Bergstrom, H. Crannell, F. J. Kline, J. T. O'Brien, J. W. Lightbody, Jr., and S. P. Fivozinsky, Phys. Rev. C 4, 1514 (1971) and references cited therein.

<sup>8</sup>I. C. Nascimento, I. D. Goldman, C. F. Wong, and H. S. Caplan, unpublished.

<sup>9</sup>The errors are based on a  $\chi^2$  vs  $Q$  (or  $b$ ) plot, assuming  $\chi^2(Q \pm \sigma_Q) = \chi^2(Q) + 1$ . In evaluating  $\chi^2(Q + \sigma_Q)$ , all remaining parameters are readjusted to obtain a new minimum. The error asymmetry results from a deviation of the  $\chi^2$  hypersurface from the usual parabolic shape as-

sociated with linear functions.

<sup>10</sup>J. A. Jansen, R. Th. Peerboom, and C. De Vries, Nucl. Phys. A188, 337 (1972).

<sup>11</sup>H. A. Bentz, R. Engfer, and W. Bühring, Nucl. Phys. A101, 527 (1967).

<sup>12</sup>M. Bouten, M. C. Bouten, H. Depuydt, and L. Schotsmans, Nucl. Phys. A127, 177 (1969).

<sup>13</sup>A. G. Blachman and A. Lurio, Phys. Rev. 153, 164 (1967).

<sup>14</sup>M. Rosen, R. Raphael, and H. Überall, Phys. Rev. 163, 927 (1967).

<sup>15</sup>E. Friedland and I. Venter, Z. Physik 243, 126 (1971).

<sup>16</sup>J. C. Adloff, K. H. Souw, and C. L. Cocke, Phys. Rev. C 3, 1808 (1971).

<sup>17</sup>J. C. Adloff, W. K. Lin, K. H. Souw, and P. Chevallier, Phys. Rev. C 5, 664 (1972).

<sup>18</sup>G. M. Griffiths, Nucl. Phys. 65, 647 (1965).

<sup>19</sup>R. Neuhausen and R. M. Hutcheon, Nucl. Phys. A164, 497 (1971).

<sup>20</sup>T. de Forest, Jr., and J. D. Walecka, Advan. Phys. 15, 1 (1966).

<sup>21</sup>M. A. Preston, *Physics of the Nucleus* (Addison-Wesley, Reading, Massachusetts, 1962), Chap. 10, p. 257.

<sup>22</sup>J. P. Davidson, *Collective Models of the Nucleus* (Academic, New York, 1968), Appendix D.